Lab on a Chip

COMMUNICATION

View Article Online
View Journal | View Issue

Cite this: *Lab Chip*, 2016, **16**, 1346

Received 20th February 2016,
Accepted 10th March 2016

DOI: 10.1039/c6lc00231e

www.rsc.org/loc

Controlled assembly of heterotypic cells in a core–shell scaffold: organ in a droplet†

Qiushui Chen,[ab] Stefanie Utech,[b] Dong Chen,[b] Radivoje Prodanovic,[c] Jin-Ming Lin*[a] and David A. Weitz*[b]

This paper reports a droplet-based microfluidic approach to fabricate a large number of monodisperse, portable microtissues, each in an individual drop. We use water–water–oil double emulsions as templates and spatially assemble hepatocytes in the core and fibroblasts in the shell, forming a 3D liver model in a drop.

Nearly all tissues are integrated three-dimensional (3D) structures of multiple types of cells and extracellular matrices (ECMs).[1,2] The function of a tissue is typically governed by multiple cues, ranging from intercellular signaling to cell interactions with the surrounding ECMs.[3–6] The liver, for example, consists of primary hepatocytes, hepatic stellate cells, Kupffer cells, endothelial cells, and fibroblasts, which are arranged in a 3D scaffold.[7] Hepatocytes alone show very low levels of liver-specific functions, because conventional two-dimensional (2D) cultures of a monolayer of these cells on a plastic dish are poor mimics of tissues found *in vivo*.[8] Therefore, improved functionality of liver tissue mimics requires the development of 3D models that consist of simplified but similar scaffolds with multiple types of cells embedded in ECMs and that express improved functionality.[9–12]

Well-defined spatial distributions of different cells in 3D architectures made of biocompatible ECMs are required to construct artificial tissues that mimic the *in vivo* microenvironment. Miniaturized, multi-well culture systems,[13–15] 3D cell printing,[16–18] and 3D cell molding[19] have each been used to develop 3D artificial liver models. In each case, hepatocytes are co-cultured with other cells in micropatterned 3D scaffolds; they are separated in space while being close enough to each other that they can interact biochemically. Therefore, different cells are able to coordinate both homotypic and heterotypic cell–cell interactions and show improved liver-specific functions.[20–22] However, these technologies are limited in terms of uniformity, portability and quantity. Versatile human microtissues composed of different cells in precisely controlled 3D structures are, as yet, unavailable.

Droplet-based microfluidics can produce monodisperse droplets whose size can be precisely controlled and whose internal structure can be tailored to incorporate different cells in designated locations.[23–26] However, previous microfluidic-based research has focused on biocompatible hydrogel microparticles templated from single water-in-oil (w/o) emulsions.[27–31] These would lead to an over-simplified 3D cellular microenvironment with limitations both in terms of impaired cell–cell contact and undefined spatial distribution of different cells in the drops. More sophisticated structures with well-defined 3D architectures are, therefore, required.

In this paper, we report the first study of reconstituting "organ in a droplet" by controlled assembly of heterotypic cells in biocompatible 3D core–shell hydrogel scaffolds. We use droplet-based microfluidics to produce highly monodisperse structures that enable multiple types of cells to be optimally arranged to create an artificial liver in a drop. We produce water–water–oil (w/w/o) double emulsions which we use as templates to successfully integrate the 3D core–shell scaffold with hepatocytes in the core surrounded by fibroblasts in the shell. We crosslink the shell of alginate hydrogel by triggered release of calcium cations; this method avoids exposure to harsh environments during fabrication and creates structures with good integrity and high permeability. The hepatocytes and fibroblasts co-cultured in the drop develop both homotypic and heterotypic cell–cell interactions, which cannot be achieved in a 2D culture system. Albumin secretion and urea metabolism, which are good assays of liver-specific

[a] *Department of Chemistry, Tsinghua University, Beijing 100084, PR China. E-mail: jmlin@tsinghua.edu.cn*
[b] *John A. Paulson School of Engineering and Applied Sciences, Department of Physics, Harvard University, Cambridge, MA 02139, USA. E-mail: weitz@seas.harvard.edu*
[c] *Faculty of Chemistry, University of Belgrade, Studentskitrg 12, Belgrade, Serbia*

† Electronic supplementary information (ESI) available: Preparation of the core–shell scaffold, controlled assembly of multiple cells into the 3D scaffold, cell viability analysis, morphology characterization and biomarker measurements. See DOI: 10.1039/c6lc00231e

functions, both exhibit higher activity in the microtissues as compared to that in hepatocytes alone.

To construct the core–shell scaffolds, we use w/w/o double emulsions as templates and generate core–shell droplets in a flow-focusing microfluidic device, as shown in Fig. 1. The inner phase is the cell culture medium and the middle phase is an alginate aqueous solution, a well-studied biocompatible polymer that shows excellent cell function and survival in the network.[32] The inner phase co-flows with the middle phase due to their low Reynolds numbers. The fluorinated carbon oil at the cross-junction forms monodisperse droplets consisting of an aqueous core and a hydrogel shell (Fig. 1b and c). Instead of crosslinking by UV exposure, which is generally harmful to cells, we introduce an additional oil flow containing 0.15% acetic acid downstream and trigger the release of Ca^{2+} from the Ca-EDTA complex in the alginate solution; the divalent Ca^{2+} ion subsequently binds to two different carboxylic groups of the alginate chains, forming a crosslinked 3D network (Fig. 1a). The *in situ* crosslinking locks alginate in the shell, which is directly visualized by fluorescence confocal microscopy by labeling alginate with fluorescein (see ESI,† Scheme S1), as shown in the inset of Fig. 1d. Using these w/w/o double emulsions as templates, we are able to fabricate a large number of monodisperse core–shell droplets with a well-controlled internal structure (diameter = 169 ± 6 μm, see ESI,† Fig. S1).

To assemble hepatocytes in the core, we suspend hepatocytes in the cell culture medium and inject them with the inner phase (see ESI,† Fig. S2). The hepatocytes are subsequently encapsulated in the core by the hydrogel shell and they start to form aggregates after several days of culture, as shown in Fig. 2a. The aggregate is a common phenotype of healthy hepatocytes and is clear proof of direct cell–cell contacts due to homotypic cell–cell interactions. Similarly, we distribute fibroblasts in the shell by premixing them with the alginate solution and injecting them with the middle phase (see ESI,† Fig. S3). The fibroblasts are then confined in the shell by the crosslinked alginate network and there are no cells observed in the core, as shown in Fig. 2b. Random co-cultures of hepatocytes and fibroblasts in the same compartment will have lower liver-specific functions due to the lost balance of homotypic and heterotypic cell–cell interactions.[13] Therefore, to mimic the 3D structure of human liver *in vivo* and to develop an artificial liver in each drop, we simultaneously assemble hepatocytes (HepG2 cells) in the core surrounded by fibroblasts (NIH-3T3 cells) in the shell, forming a spheroid of different cells embedded in a 3D ECM (see ESI,† Fig. S4 and Movie S1). In our study, the heterocellular spheroids are generated by one-step *in situ* crosslinking of alginate in the shell, after which the spheroids are quickly transferred to the cell culture medium. The exposure of cells to mild acidic conditions during the whole process is limited and has little effect on the viability of cells, as evidenced by the predominance of live cells (green) and the complete lack of any dead cells (red) in the live–dead assay, as shown in Fig. 2c.

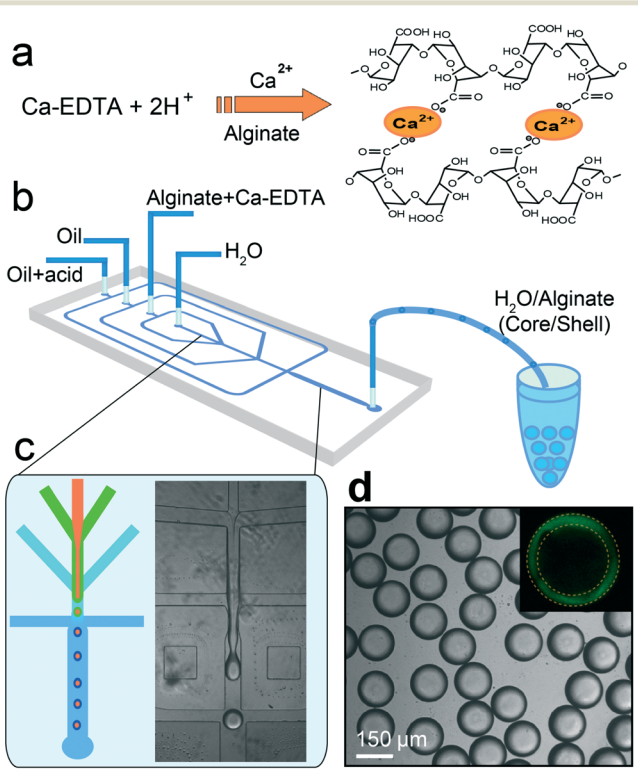

Fig. 1 Construction of the 3D scaffold in a drop consisting of an aqueous core and a hydrogel shell. a) Crosslink of the alginate network by triggered release of Ca^{2+} from the Ca-EDTA complex. b) Schematic diagram of the PDMS device. c) Fabrication of core–shell droplets using w/w/o double emulsions as templates. Alginate in the shell is crosslinked by *in situ* triggered release of Ca^{2+}. d) Monodisperse core–shell droplets generated using the droplet-based microfluidics. The shell of alginate hydrogel is clearly identified under a confocal microscope when alginate is labeled with fluorescein, as shown in the inset.

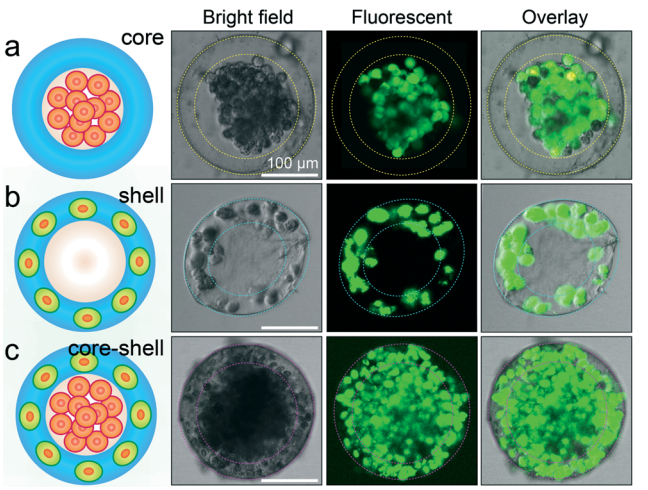

Fig. 2 Spatial assembly of different cells in the 3D core–shell scaffold. a) HepG2 cells confined in the core by the hydrogel shell. b) NIH-3T3 fibroblasts immobilized by the crosslinked alginate network in the shell. c) Simultaneous assembly of hepatocytes in the core and fibroblasts in the shell, forming an artificial liver in a drop. Cell viability is characterized by the calcein AM/EthD-1 staining kit. The scale bars are 100 μm.

We culture the core–shell spheroids in the medium at 37 °C. The spheroids maintain their spherical shape even for two weeks of culture, during which time the cells have grown denser, as shown in Fig. 3a–c. The distinct spherical shape is also observed in freeze-dried samples using scanning electron microscopy, as shown in Fig. 3d and magnified in Fig. 3e. Moreover, the cross-section of a freeze-dried spheroid reveals dense cell aggregates in the core and dispersed cells in the shell, as shown in Fig. 3f. These observations suggest that the hydrogel shell of crosslinked alginate is mechanically strong. This strength, together with the portability of each microtissue in a drop, enables us to store them at −80 °C, thaw them at 37 °C and culture them again without destroying the structure or affecting the viability of the cells, as shown in Fig. 3g. While the shell of alginate hydrogel is robust, it is also highly permeable, enabling nutrients and metabolites to pass through; therefore, the cells in the spheroids can be cultured for long periods of time, as evidenced by the high viability of the cells cultured in the spheroids. After 10 days of culture, the cells are predominantly live (green) and there is a complete lack of dead cells (red), as revealed by the live–dead staining kit (Fig. 3h). During this period, the cells have grown denser. However, because the cells can't attach to the unmodified alginate network, they can't migrate from one layer to the other over time. Therefore, the hepatocytes and fibroblasts remain spatially separated, which is beneficial for their liver-specific functions. Even after 14 days, a slight decrease in cell viability is observed; the percentage of dead cells is about 34%, as shown in Fig. 3i. It is possible that a hypoxic core developed at day 14 due to cell proliferation and the resulting high cell density.

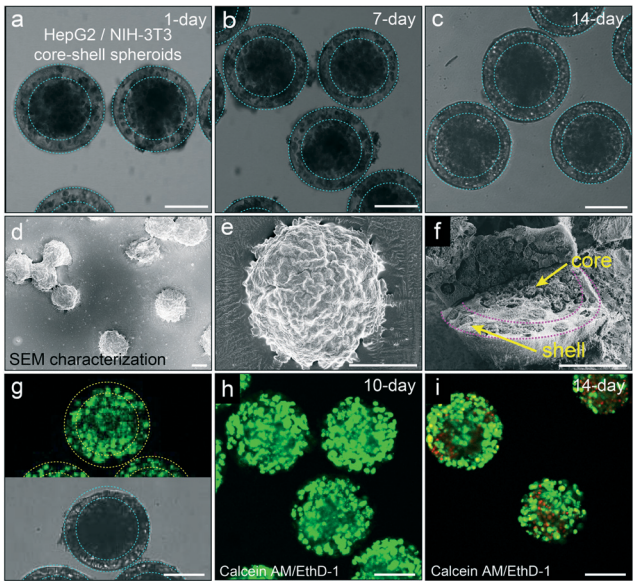

Fig. 3 Co-culture of hepatocytes and fibroblasts in the core–shell spheroids. Morphology of the heterocellular spheroids and viability of the cells in the hydrogel scaffold. a–c) Co-culture of hepatocytes in the core and fibroblasts in the shell for 1 day, 7 days and 14 days, respectively. The heterocellular spheroids maintain their spherical morphology over time. d) SEM image and e) magnified image showing individual spheroids that maintain their structural integrity after freeze-drying. f) Spatially confined cell ensembles in the core–shell structure. g) High viability of cells encapsulated in the spheroids after being frozen at −80 °C for two weeks and then thawed at 37 °C. Cells are predominantly live (green) and there is a complete lack of dead cells (red). h) Co-culture of cells encapsulated in the spheroids for 10 days showing high cell viability. i) The viability of cells cultured for 14 days decreases slightly, as evidenced by the appearance of dead cells (red). Cell viability is characterized by the calcein AM/EthD-1 staining kit. The scale bar is 100 μm in all images.

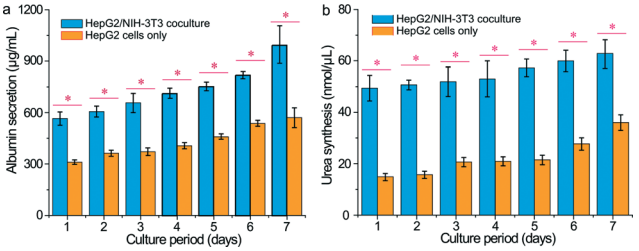

Fig. 4 Comprehensive assays of the liver-specific functions of hepatocyte/fibroblast co-culture and hepatocyte culture. a) Albumin secretion and b) urea synthesis of HepG2/NIH-3T3 co-culture and HepG2 culture measured over seven days. The liver-specific functions enhanced by the co-culture of hepatocytes and fibroblasts in the 3D core–shell spheroids are statistically significant ($*p < 0.01$).

To measure the liver-specific functions of the microtissues in a drop, we monitor their albumin secretion and urea synthesis over time; these two metabolites are key biomarkers of the liver and these assays have been widely used in drug screening.[33] We culture two samples with the same amount of hepatocytes, one in the core–shell structure with fibroblasts in the shell and the other without fibroblasts, and monitor the concentration of albumin and urea in the medium using albumin and urea assay kits, respectively. Compared to the monotypic culture of hepatocytes alone, the co-culture of hepatocytes and fibroblasts in the core–shell spheroids displays both increased albumin secretion and urea synthesis, as shown in Fig. 4a and b. The enhanced liver-specific functions substantially differentiate our 3D microscale co-culture from the conventional monotypic cell culture (statistically significant, $*p < 0.01$). These results suggest that the co-culture of hepatocytes and fibroblasts embedded in the 3D core–shell scaffold is a good model of the liver *in vitro* and has a balance of homotypic and heterotypic cell–cell interactions, which are beneficial for the expression of their liver-specific functions. High-throughput assays of human tissue responses using these uniform, portable microtissues, each in a drop, will be valuable for rapid assessment of drugs, chemicals and cosmetics.

Conclusions

We use droplet-based microfluidics and hierarchically assemble hepatocytes and fibroblasts into a 3D core–shell scaffold, forming an artificial liver in each drop. The strong mechanical properties and high permeability of the hydrogel shell enable the cells in the spheroids to be cultured for long periods

of time. Within the optimized microscale structure that promotes both homotypic and heterotypic cell–cell interactions, the co-culture of hepatocytes in the core surrounded by fibroblasts in the shell successfully expresses high-level liver-specific functions. Thousands of monodisperse microtissues, each in an individual drop, are achievable using this microfluidics technology, and each maintains enhanced liver-specific functions. In addition, hepatocytes and fibroblasts can be easily replaced with other cells to construct other tissue models and study cell-to-cell interactions in general. Thus, these structures are a promising *in vitro* liver model for high-throughput drug screening assays.[34,35]

Acknowledgements

Q. Chen acknowledges the China Scholarship Council (2012[3013]) and the staff of *Experimental Soft Condensed Matter* at Harvard University. This work was financially supported by the National Natural Science Foundation of China (no. 214350002, 91213305, and 81373373) and the China Equipment and Education Resources System (no. CERS-1-75). This work was also supported by the National Science Foundation (DMR-1310266), the Harvard Materials Research Science and Engineering Center (DMR-1420570) and the National Institutes of Health (R01EB014703). S. Utech was supported by Deutsche Forschungsgemeinschaft.

References

1 E. S. Place, N. D. Evans and M. M. Stevens, *Nat. Mater.*, 2009, **8**, 457–470.
2 J. M. Grolman, D. Zhang, A. M. Smith, J. S. Moore and K. A. Kilian, *Adv. Mater.*, 2015, **27**, 5512.
3 V. Vogel and M. Sheetz, *Nat. Rev. Mol. Cell Biol.*, 2006, **7**, 265.
4 W. P. Daley, S. B. Peters and M. Larsen, *J. Cell Sci.*, 2008, **121**, 255.
5 F. Klein, B. Richter, T. Striebel, C. M. Franz, G. von Freymann, M. Wegener and M. Bastmeyer, *Adv. Mater.*, 2011, **23**, 1341.
6 T. P. Kraehenbuehl, R. Langer and L. S. Ferreira, *Nat. Methods*, 2011, **8**, 731.
7 Z. Kmieć, *Adv. Anat., Embryol. Cell Biol.*, 2001, **161**, 1.
8 X. Gidrol, B. Fouque, L. Ghenim, V. Haguet, N. Picollet-D'hahan and B. Schaack, *Curr. Opin. Pharmacol.*, 2009, **9**, 664.
9 F. T. Moutos, L. E. Freed and F. Guilak, *Nat. Mater.*, 2007, **6**, 162.
10 S. F. Wong, D. Y. No, Y. Y. Choi, D. S. Kim, B. G. Chung and S. H. Lee, *Biomaterials*, 2011, **32**, 8087.
11 Q. Chen, J. Wu, Q. C. Zhuang, X. X. Lin, J. Zhang and J.-M. Lin, *Sci. Rep.*, 2013, **3**, 2433.
12 J. El-Ali, P. K. Sorger and K. F. Jensen, *Nature*, 2006, **442**, 403.
13 S. R. Khetani and S. N. Bhatia, *Nat. Biotechnol.*, 2008, **26**, 120.
14 Y. Nakao, H. Kimura, Y. Sakai and T. Fujii, *Biomicrofluidics*, 2011, **5**, 022212.
15 B. J. Kane, M. J. Zinner, M. L. Yarmush and M. Toner, *Anal. Chem.*, 2006, **78**, 4291.
16 M. Matsusaki, K. Sakaue, K. Kadowaki and M. Akashi, *Adv. Healthcare Mater.*, 2013, **2**, 534.
17 S. V. Murphy and A. Atala, *Nat. Biotechnol.*, 2014, **32**, 773.
18 J. O. Hardin, T. J. Ober, A. D. Valentine and J. A. Lewis, *Adv. Mater.*, 2015, **27**, 3279.
19 Y. T. Matsunaga, Y. Morimoto and S. Takeuchi, *Adv. Mater.*, 2011, **23**, H90.
20 A. Khademhosseini, R. Langer, J. Borenstein and J. P. Vacanti, *Proc. Natl. Acad. Sci. U. S. A.*, 2006, **103**, 2480.
21 B. Guillotin and F. Guillemot, *Trends Biotechnol.*, 2011, **29**, 183.
22 C. H. Cho, J. Park, A. W. Tilles, F. Berthiaume, M. Toner and M. L. Yarmush, *BioTechniques*, 2010, **48**, 47.
23 C. Kim, S. Chung, Y. E. Kim, K. S. Lee, S. H. Lee, K. W. Oh and J. Y. Kang, *Lab Chip*, 2011, **11**, 246.
24 S. Utech, R. Prodanovic, A. S. Mao, R. Ostafe, D. J. Mooney and D. A. Weitz, *Adv. Healthcare Mater.*, 2015, **4**, 1628.
25 H. N. Joensson and H. A. Svahn, *Angew. Chem., Int. Ed.*, 2012, **51**, 12176.
26 D. M. Headen, G. Aubry, H. Lu and A. J. García, *Adv. Mater.*, 2014, **26**, 3003.
27 M. T. Guo, A. Rotem, J. A. Heyman and D. A. Weitz, *Lab Chip*, 2012, **12**, 2146.
28 T. Rossow, J. A. Heyman, A. J. Ehrlicher, A. Langhoff, D. A. Weitz, R. Haag and S. Seiffert, *J. Am. Chem. Soc.*, 2012, **134**, 4983.
29 R. Novak, Y. Zeng, J. Shuga, G. Venugopalan, D. A. Fletcher, M. T. Smith and R. A. Mathies, *Angew. Chem., Int. Ed.*, 2011, **50**, 390.
30 D. Steinhilber, T. Rossow, S. Wedepohl, F. Paulus, S. Seiffert and R. Haag, *Angew. Chem., Int. Ed.*, 2013, **52**, 13538.
31 L. Yu, S. M. Grist, S. S. Nasseri, E. Cheng, Y.-C. E. Hwang, C. Ni and K. C. Cheung, *Biomicrofluidics*, 2015, **9**, 024118.
32 A. D. Augst, H. J. Kong and D. J. Mooney, *Macromol. Biosci.*, 2006, **6**, 623.
33 B. E. Uygun, A. Soto-Gutierrez, H. Yagi, M.-L. Izamis, M. A. Guzzardi, C. Shulman, J. Milwid, N. Kobayashi, A. Tilles, F. Berthiaume, M. Hertl, Y. Nahmias, M. L. Yarmush and K. Uygun, *Nat. Med.*, 2010, **16**, 814.
34 E. W. Esch, A. Bahinski and D. Huh, *Nat. Rev. Drug Discovery*, 2015, **14**, 248.
35 Q. Chen, Z. He, W. Liu, X. Lin, J. Wu, H. Li and J.-M. Lin, *Adv. Healthcare Mater.*, 2015, **4**, 2291–2296.